Journal of Thermal Engineering
https://jten.yildiz.edu.tr/
https://doi.org/10.47481/jten.0085

RESEARCH ARTICLE

Experimental and numerical study on thermal comfort and dynamic homogenization for heating, ventilation, and air conditioning applications using multi-jet diffusers

N. Zahout[1], A. Khelil[2,*], M. Braikia[3], H. Naji[4]

[1]University of Chlef, Laboratory of Control, Testing, Measurement and Mechanical Simulation, B. P. 151, 2000 Chlef, Algeria
[2]University of Chlef, Laboratory of Control, Testing, Measurement and Mechanical Simulation, B. P. 151, 2000 Chlef, Algeria
[3]University of Chlef, Laboratory of Control, Testing, Measurement and Mechanical Simulation, B. P. 151, 2000 Chlef, Algeria
[4]Univ. Artois, Univ. Lille, IMT Lille-Douai, Junia, ULR 4515 – LGCg, Technoparc Futura, F-62400 Béthune, France

Abstract

Jet mixing ventilation using air is a well-known technology for providing thermal comfort in indoor environments. Jet diffusers are designed to maximize the effective dispersion of clean air and thermal energy for air conditioning or heating in an inhabited room. Jet diffusers are designed to improve mixing between jets and surrounding air and take aspects of aesthetic into account. However, the existing studies mainly focus on single jets or conventional multi-jet diffusers, and few studies have examined how central jet shape affects heat comfort and dynamic homogeneity. This paper presents a novel comparison of two multi-jet diffuser configurations. Both configurations consist of six peripheral jets of similar geometry, but the central jet is designed differently, one with a lobed central jet and the other with a swirling central jet. The originality of this work lies in the systematic evaluation of these diffuser designs from experimental and numerical points of view, concerning their influence on dynamic homogenization and thermal comfort. This work is different from earlier studies in that it uses multiple turbulence models, such as the RNG k-ε, the standard k-ω, the (k-ω) SST and the RSM models to decide the best predictive method for jet interactions. It was found that the swirling diffuser improves thermal comfort and dynamic homogenization significantly without any increase in the pressure drop and sound pressure level as compared to the lobed diffuser. Quantitative results show that the swirling central jet improves the axial dynamic and thermal homogenization by about 20% and the radial dynamic and thermal homogenization by about 10% with respect to the lobed configuration. Furthermore, the present study shows that the Shear Stress Transport k-ω SST model can accurately predict the complex flow structures and thermal characteristics of multi-jet diffusers, which can be a useful tool to optimize the geometric parameters of lobed and swirling perforated panels in heating, ventilation, and air conditioning systems. Also, the k-ω SST model showed better agreement with experimental data with root mean square error values of 0.0368 for axial velocity and 0.0384 for axial temperature. The results offer new insights into diffuser design strategies for better indoor air distribution and energy efficiency.

Keywords: Mixing, ventilation, thermal homogenization, multiple-jet, turbulence models, CFD

Cite this article as: Zahout, N., Khelil, A., Braikia, M., & Naji, H. (2026). Experimental and numerical study on thermal comfort and dynamic homogenization for heating, ventilation, and air conditioning applications using multi-jet diffusers. Journal of Thermal Engineering, 12(6), 2086–2099. https://doi.org/10.47481/jten.0085

1. Introduction

This section should provide a clear background, the rationale for the study, and a comprehensive literature review. State the aims of the work clearly at the end of this section. The enhancement of the performance of devices and processes in many industrial sectors requires heat transfer efficiency. This has improved techniques such as longer fins, special heat sinks, fluid modifications, jet patterns, etc. [1-4]. A multiple jet configuration is the emission of two or more jets from a common exit plane. The jets are spaced a distance apart. The reasons for these setups. They improve the mixing and help in reducing the jet noise, which is important to meet stringent noise requirements. Many high-performance airplanes have different jet configurations. These designs generally employ booster rockets beneath the wings to aid take-offs from shorter

*Corresponding Author
E-mail Adress: a.khelil@univ-chlef.dz

Submitted: 24 January 2025; **Accepted:** 24 January 2025

This paper was recommended for publication in revised form by Editor-in-Chief Ahmet Selim Dalkılıç

Published by Yıldız Technical University, İstanbul, Türkiye
This is an open access article under the CC BY-NC license (http://creativecommons.org/licenses/by-nc/4.0/).

runways. Multiple jets are involved in many applications. A significant part of rocket engine exhaust plumes with strap-on boosters. These technologies are also widely used in film-cooling applications to the walls of combustion chambers [5-11], turbine blades, and re-entry vehicle nose cones. Besides, the micro-blowing technique is meant to reduce the skin friction drag and it is made of many jets. Many practical applications also employ multiple jets such as heating, ventilation and air conditioning, glass shaping, tempering, paper processing and textile drying. However, current research focuses mainly on single jets or standard multi-jet diffusers. Moreover, minimal study has been conducted about the influence of central jet shape on thermal comfort and dynamic uniformity.

In this paper, a new comparison is made between two configurations of a multi-jet diffuser with six peripheral jets of similar geometry but different core jet shape, one with a lobed central jet and the other with a swirling central jet. The particularity of this study is the complete experimental and numerical assessment of various diffuser designs about their impact on dynamic homogeneity and thermal comfort. The present study differs from the earlier studies in that it includes different turbulence models, for instance, the RNG k-ε, the k-ω SST, the standard k-ω, and the RSM models. To see what the best way is to forecast jet interactions the most correct. As part of their research, Meslem et al. [12] investigated twin cross-jets and compared them to twin circular jets while keeping the same starting Reynolds number and separation distance. The cross-lobed jet interactions are more efficient and occur earlier than the circular jet interactions. The lobes produced a flow rate 3 times higher than the circular twinjet. In addition, the cross-jet arrangement led to more uniform flow distribution and longer reach for both twinjet and row jet configurations. Nastase and Meslem [13] investigated the effect of vortex dynamics on induction in the first regions of circular and lobed jets issuing from a lobed nozzle. Their study highlighted the significant role played by longitudinal structures throughout the induction procedure. About circular jets, the induction was strongly dependent on the occurrence of the Kelvin-Helmholtz ring structures. In the lobed jets this effect was not so important. In another work, Meslem et al. [14] studied the induction enhancement of two-lobed jets over a normal circular jet with a constant flow rate and nozzle size. Three types of nozzles have been tested: a circle reference, a straight uninclined lobed and a double-inclined lobed nozzle. The second nozzle gave an improvement in induction up to four times greater, the first nozzle giving about 70 % of this improvement. Sajadi et al. [15] carried out a numerical simulation of airflow in swirling diffusers. A parametric study was carried out to explore the impact that geometric parameters have on the productivity and efficiency of the diffuser induction. This was done to find out about this effect. The results clarified the effect of diffuser geometry on flow behavior and mixing performance. Nastase et al. [16] applied the Draft Risk (DR) index to evaluate what effect a square air propagation grid with lobed fins has on the comfort of the ambient space that surrounds it. This grid showed an increase in the DR values in populous areas, different to standard straight-wing grids. Bennia et al. [17] tested several nozzle designs for efficiency of performance. The examination of the jet axial velocity profiles proves that the diffuser with angled lobes eases a more uniform flow. In a related study, Bennia et al. [18 and 19] recommended the use of lobed diffusers to improve air dispersion in buildings. The numerical results of RNG k-ε and k-ω SST models were well matched with the experimental data. These results show possible uses of lobed jets in residential HVAC systems. Xu et al. [20] examined the flow behaviors of jet pumps with different nozzle geometric shapes by the Realizable k-ε model and finite volume method. They found that the use of non-circular nozzles decreased the recirculation zones and the frictional losses and increased the mixing efficiency. The flow and temperature fields for different jets on a heated plate were investigated by Draksler et al. [21] using an LES model. They found that heat transfer was governed by convective cooling due to tangential flow and quasi-periodically by severe quenching due to large scale vortices. Radhouane et al. [22] performed simulations of two inclined elliptical jets issuing non-reactive smoke into a cooler uniform flow. The turbulence modeling was done by using finite volume approach with Reynolds Stress Model (RSM). The mixing and dynamics of jets have been studied extensively in applications such as ventilation, heating and air-conditioning systems. The velocity profiles were broader at higher temperature, with an increase in jet dispersion and flow field homogeneity. Medaouar et al. [23] studied experimentally and numerically a core lobed jet with six peripheral lobes. The researchers discovered that jet mixing altered the velocity and temperature inside the mixing zone, resulting in enhanced dispersion. Simulations were performed according to RANS equations with k-omega SST model. OpenFOAM code was used by Kannan and Panchapakesan [24] to simulate a maximum of five individual circular jets. It has been proved via the results that the standard k-ε model is capable of properly recreating the main flow characteristics. These characteristics include the reduction in axial velocity, secondary flows, flow entrainment and turbulent kinetic energy. Depuru Mohan et al. [25] similarly investigated mixing in single lobed and multiple jet configurations (circular and lobed) using the k-ε model at identical flow rates. Temperature was a passive scalar. They found that the lobed jets provided better mixing because of their shorter core lengths and higher entrainment velocities. The steady momentum flux between the jets also enhanced overall mixing. The thermal comfort and the airflow behavior of a ceiling-mounted three-cone diffuser with lobes was studied by Bragança et al. [26]. This arrangement provided improved comfort without increasing the pressure loss or energy consumption compared to conventional diffusers in heating conditions. Khelil et al. [27] studied asymmetrically disposed swirling jets with first and second order turbulence models. It was found that the RSM model could capture the mean flow features better. Swirling jet interactions improved the temperature distribution and jet propagation near the blowing diffusers. Braikia et al. [28] investigated different swirling jet configurations to enhance thermal homogeneity by varying the position of air-blowing sources. In their results the central jet was important to get consistent temperature dispersion.

The main findings of their study were:

- In twin swirling jet configurations, the spacing between blow orifices varied to reduce the radial temperature differences. It also enhanced jet spreading and thermal homogenization. Moreover, the spacing was changed dynamically, which resulted in lower blowing velocities, delayed jet merging and higher fluctuation intensity.
- The decline in temperature for multiple swirling jets (3 and 4 jets) arranged in a triangular configuration was significantly less than that compared to single jets.
- This occurred because of the interaction that took place between the center jet and the boundary jets that were in proximity to it. The interaction enhanced the mixing and resulted in a more homogeneous temperature gradient.
- In the far-field region a significant change of flow behavior was seen. The formation of seven spinning jets was particularly effective. In this paper, the velocity and temperature profiles of two different jet designs are presented. The first configuration is a center-lobed jet and six equally spaced peripheral-lobed jets. The second configuration consists of a core swirling jet encircled by six equidistant lobed jets. Both the configurations are tested with ANSYS-CFD. The analysis is concerned with their possible application in systems of domestic ventilation, heating and air-conditioning.

2. Experimental method

The experiments were conducted in a specialized facility designed to study multiple impinging lobed jets, as depicted in Figure 1. The setup was housed in a controlled environment within a room measuring 3.9 m × 3.75 m × 2.95 m (L × W × H), ensuring insulation from external disturbances to keep a stable ambient temperature. The configuration included a frame equipped with a device to direct hot air downward, with the arrangement of diffusers varying based on the specific configuration under examination. Velocity and temperature measurements were obtained using a VelociCalc Plus Model 8385A multifunctional thermo-anemometer, which features a probe capable of capturing parameters such as pressure, velocity, and temperature. The measurements were displayed or recorded via a computer for later statistical analysis. The thermal sensor's temperature measurement accuracy was ±0.1 °C, and the velocity accuracy was ±0.015 m/s. The probe was mounted on rods that allowed vertical and horizontal movement, enabling comprehensive axial and radial temperature and velocity measurements. Additionally, a digital thermometer placed outside the experimental room provided real-time readings of the ambient temperature (Ta).

The experimental setup was carefully designed to ensure precise and reliable data collection, supporting later numerical and analytical investigations. All experiments were performed under uniform heat flow conditions, keeping a Reynolds number of approximately 2×104 for each diffuser. The jet outlet temperature was consistently set at 363 K, and the first axial jet velocity was kept at 8 m/s. The study focused on a multi-jet system forming two distinct configurations, according to the information shown in Table 1.

Table 1. Studied configurations

Configuration 1	Seven air jet diffusers with lobed geometry, one of which is central and six peripherals.
Configuration 2	Six peripheral air jet diffusers with lobed geometry and a central diffuser with swirling geometry.

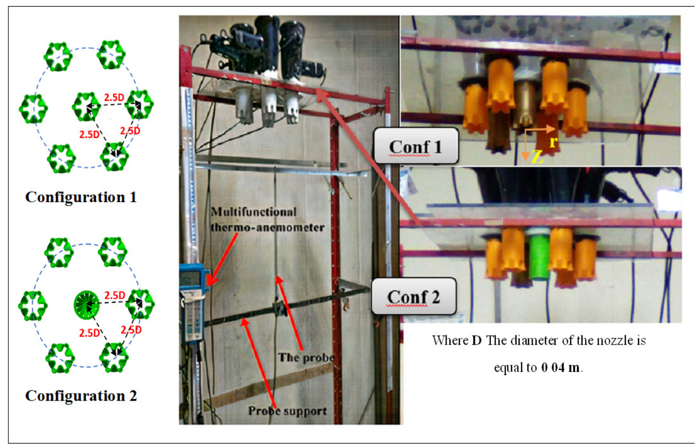

Figure 1. Experimental setup

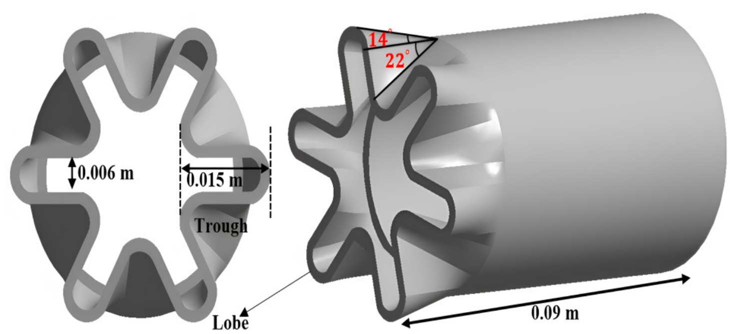

Figure 2. The lobed diffuser

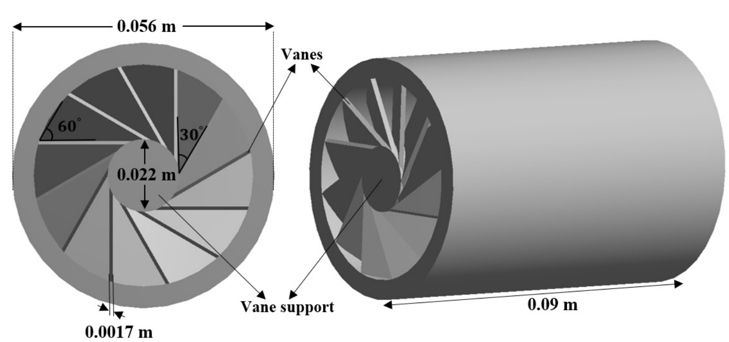

Figure 3. The swirling diffuser

The design specifications of the lobed diffusers used in this investigation are depicted in Figure 2. Each diffuser has a circular tube with a 40 mm diameter and a daisy-shaped exit. A total of 6 sinusoidal troughs and 6 inclined lobes with parallel faces are included in the exit plane. The internal penetration angle (θint) is 22°, while the external penetration angle (θout) is 14°. There are 15 millimeters of length and 6 millimeters of height in each of the lobes. Figure 3 shows a swirl nozzle consisting of twelve aluminum vanes mounted on an aluminum holder with a diameter of 0.022 meters. The vanes are positioned at specific inclination angles to induce a vortex effect: the first set of vanes is inclined at 30° relative to the jet axis, and the second set is inclined at 60° relative to the flow plane.

3. Numerical simulations

3.1. Solution procedure

The solution method employs ANSYS Fluent for conducting turbulence simulations. The control volume approach is used to solve the three-dimensional Navier-Stokes equations, incorporating the effects of pressure, temperature, and turbulence. An implicit pressure-based solver is implemented, with the SIMPLE algorithm applied for pressure-velocity coupling.

3.2. Mathematical modeling

In this study, overbars or capital letters are Reynolds-averaged quantities, while primes or lowercase letters show fluctuating components. The dimensionless form of the Reynolds-averaged governing equations, applicable to steady and incompressible flow, is provided below [36-40]:

$$\frac{\partial U_i}{\partial x_i} = 0, \tag{1}$$

$$\rho\frac{\partial (U_i U_j)}{\partial x_j} = -\frac{\partial P}{\partial x_i} + \frac{\partial}{\partial x_j}\left[\mu\left(\frac{\partial U_i}{\partial x_j} + \frac{\partial U_j}{\partial x_i}\right) - \overline{\rho u_i' u_j'}\right] \tag{2}$$

$$\rho C_p U_i \frac{\partial T}{\partial x_i} = \frac{\partial}{\partial x_i}\left[\lambda\frac{\partial T}{\partial x_i} - \rho C_p \overline{u_i' T'}\right] \tag{3}$$

where Ui and T are the average velocity and temperature, respectively; u_i', u_j' and T' are the fluctuation components; $-\rho\overline{u_i' u_j'}$ and $-\rho C_p \overline{u_i' T'}$ corresponds to the mean Reynolds stresses and turbulent heat fluxes that must be modelled to get the equations to a conclusion that may be considered definitive. An exact expression of the Boussinesq hypothesis may be found in the following equation. This hypothesis sets up a connection between the average velocity gradients and Reynolds stresses.

$$-\rho\overline{u_i' u_j'} = \mu_t\left(\frac{\partial U_i}{\partial x_j} + \frac{\partial U_j}{\partial x_i}\right) - \frac{2}{3}\left(\rho k + \mu_t\frac{\partial U_i}{\partial x_i}\right)\delta_{ij} \tag{4}$$

In this equation, turbulent kinetic energy is denoted by the symbol k.

$k = \frac{1}{2}\overline{u_i' u_i'}$, and δ_{ij} is the identity of the tensor. The Boussinesq method has several advantages, one of which is that the computation of the turbulent viscosity involves a relatively low computing cost. It is problematic in that it presumes that is an isotropic scalar variable which is not necessarily the case. The k-ε model is an equation model based on the Boussinesq assumption.

Here, four turbulence models: k-ω Standard model, k-ω SST model RNG k-ε model and the RSM model, have been employed [29-35].

4. CFD simulations

4.1. Meshing and calculation domain

In general, the choice between hexahedral and tetrahedral grids depends on the complexity of the domain. In this study, a tetrahedral mesh was selected to accommodate the intricate geometry of the nozzles (refer to Figure 4). It's important to highlight that generating a structured grid might pose challenges and consume a significant quantity of time. Consequently, the use of unstructured grids is considered as an alternative. While this approach may lead to increased memory usage, it is well-suited for accurately being complex domains, such as the one under consideration in this study.

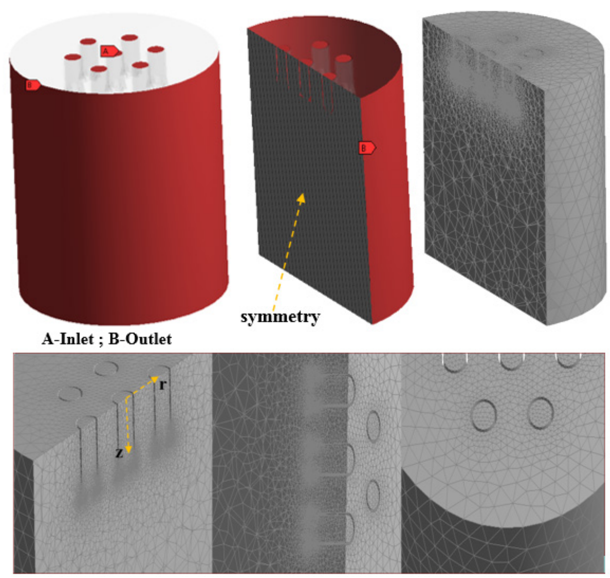

Figure 4. Computational domain meshing

4.2. Mesh size independence

Before starting the simulations, it is imperative to set up a proper grid density to ensure correct results. The grid resolution is decided through a grid-sensitivity analysis employing four different grids, ranging from coarse to fine (refer to results in Figure 5 and details in Table 2) [36]. The analysis is streamlined using the k-ω SST model. Figure 5 illustrates a comparison of the four grid densities (mesh 1 to mesh 4), with the corresponding number of cells highlighted in bold in Table 2. Notably, grids 1 and 2 exhibit considerable variations in results compared to grids 3 and 4. It's essential to emphasize that this grid-sensitivity analysis was replicated for configuration 2.

Following the evaluation of outcomes, Grid 3 was chosen for later numerical simulations. It is worth mentioning that the selected meshes' wall coordinate y+ values are less than one, and the convergence requirement for the calculated residues is less than for turbulent energy and for every other parameter. This figure also illustrates the axial development of the mean velocity U. As predicted, each design has a suitable density. Consequently, the remaining part of the study, an individual grid was chosen for each configuration since it provides a precise resolution and any increase in mesh density has no effect on the quality of the results. As a result of this, based on the data, it has been determined that increasing the mesh density does not have any effect whatsoever on the quality of the results.

Table 2. Tested meshes

	Configuration 2	Configuration 1
Mesh 1	1121713	1432484
Mesh 2	2008829	2364726
Mesh 3	**3548113**	**3157363**
Mesh 4	4427238	4630112

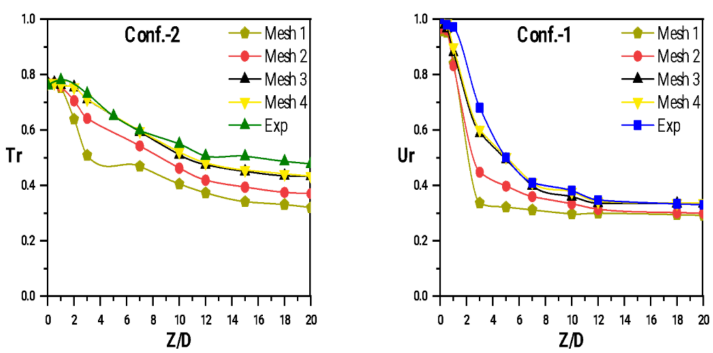

Figure 5. Mesh effect for the axial velocity of configuration 1 and axial temperature of configuration 2 with the k-ω SST model

4.3. Boundary conditions

Listed below is a compilation of the boundary conditions that were developed for the turbulence models that were used in this investigation:

- Inlet velocity: 8 (m / s)
- Inlet temperature (K) 363.
- Turbulence intensity: 5 (%).
- Reynolds number: 20000
- Convergence criteria: Energy $=10^{-6}$, other parameters = 10^{-4}

4.4. Solution approach

In our calculations, we applied continuity, momentum, energy, and turbulence equations as governing principles. Utilizing the CFD software ANSYS Fluent [41] and the SIMPLEC algorithm, we supposed that the air flow was steady, incompressible and turbulent. A verified inlet Mach number below 0.3 confirms this assumption. The transport equations' diffusion terms were approximated using a central second-order difference, while advection terms were managed through a second-order upwind numerical scheme. Convergence was set up by monitoring global residuals, with the solution considered reliable when these residuals decreased by over five orders of magnitude, and the quantities of interest reached steady-state values.

5. Results and discussion

5.1. Experimental analysis

In the first segment, our focus is on presenting the experimental results related to the dimensionless temperature $T_r = (T_i - T_a)/(T_{max} - T_a)$ and velocity $(U_r = U_i/U_{max})$ (obtained from studying the interaction of seven free lobed jets (forming a central jet and six surrounding jets) forming two distinct configurations. It is essential to highlight that measurements of axial and radial temperature, as well as velocity, were taken in both the main and radial directions. A detailed comparison of these profiles for the two configurations is shown to illustrate the influence of the center jet in relation to the surrounding jets on the dynamics and thermal characteristics.

5.2. Numerical simulation

In the next section we present the numerical simulation of the two above-mentioned set-ups. This also includes the use of the previously described RANS models. A quick description of these models is given to evaluate their respective efficiency. The numerical simulation is intended to complement and confirm the experimental results and to make a significant contribution to a comprehensive understanding of the flow dynamics and thermal performance within the researched configurations.

5.3. Experimental results

5.3.1. Axial profiles of temperature and velocity

The axial distribution of reduced velocity and temperature for two identical setups having similar nozzle sizes and operating circumstances are shown in Figure 6. These profiles show the fluctuations of the velocity and the temperature along the axial line from the outflow of the nozzle. The profile comparison between setups shows some changes in the behavior of the velocity and temperature along the axial direction. The axial station (Z/D) can be used to classify the flow features of an axial jet into three regions: Velocity and temperature are constant from the nozzle exit to the jet diameter. Jets are not interwoven, remain autonomous. Further downstream Z/D = 2, the axial velocity reduces rapidly, and the temperature reduces to 7 jet diameters. A transfer of energy from the axially direction to the radially direction is carried out via the jet interplay causing mixing and dispersion, which reduces velocity and temperature. Beyond Z/D > 7, the gradients in velocity and temperature decrease, suggesting stabilization. Profiles are not so accentuated to suggest a flow evolution towards a stationary state with little axial velocity and temperature variations. Comparing the configurations, configuration 2 has a faster drop of axial velocity than configuration 1 at any axial location. The reduction in velocity as well as temperature is a sign of a radial transfer of energy implying stability and homogeneity of the ensuing flow parameters away from the jet source. The reduction of axial velocity is mainly due to the higher turbulent mixing and the jet expansion. In the present configuration, the swirling jet at the center induces quick entrainment of ambient air hence increasing turbulent diffusion and leading to a faster decay of the axial momentum. The interaction that occurs between the swirling central jet and the adjacent lobed jets promotes shear layer production, hence enhancing velocity decay along the jet axis.

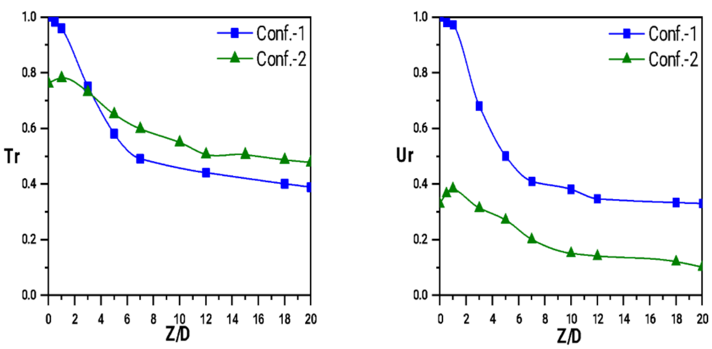

Figure 6. Experimental velocity and temperature profiles in the axial direction

5.3.2. Radial profiles of velocity

Figure 7 presents the measured radial velocity profiles along the Z direction for six different axes (Z/D = 1, 3, 5, 7, 12, 18). It is seen that the highest and lowest velocities, near the diffuser exit, display sharp peaks and troughs near the blowing surface (Z/D ≤ 7). When the minimum velocity is induced, a recirculation zone forms near the exit of the diffusers (at smaller axial stations, Z/D ≤ 7). The jets begin the mixture at the axial station Z/D = 3, and the decrease in maximum values is balanced by an increase in the lowest values. Once Z/D = 12 is reached, the velocity profiles begin to stabilize, resembling those of a single jet.

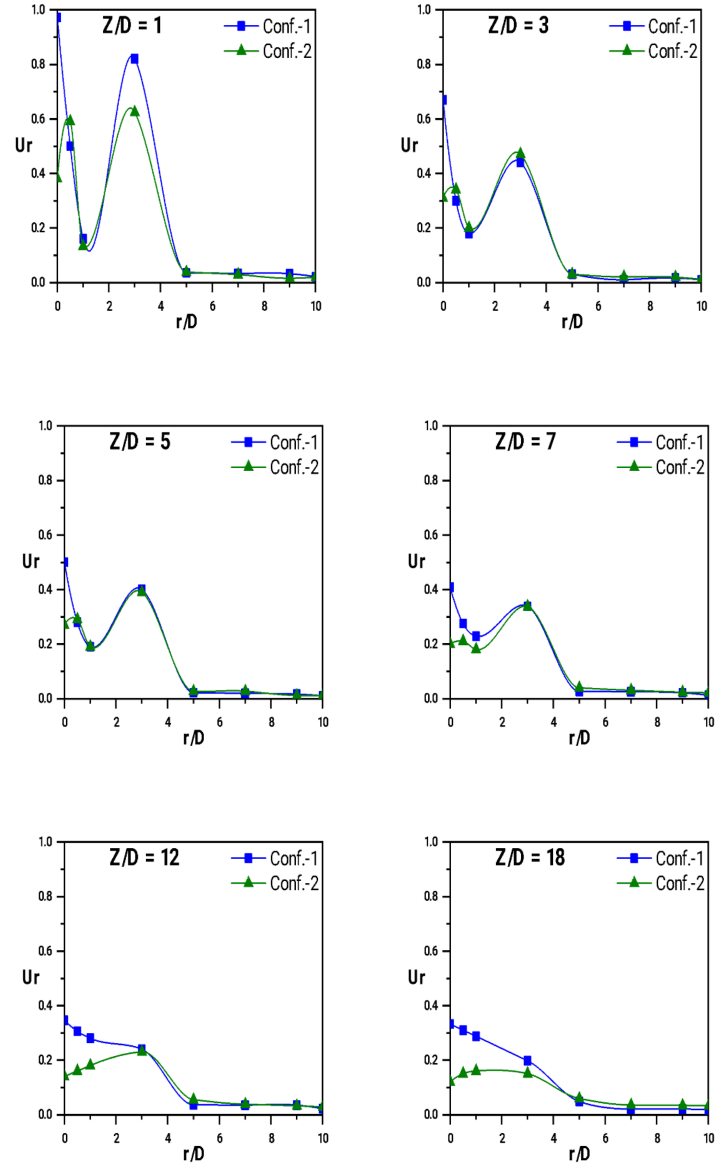

Figure 7. Experimental radial velocity profiles

5.3.4. Radial profiles of temperature

Figure 8 shows the radial temperature profiles measured along the Z direction for six different axes (Z/D = 1, 3, 5, 7, 12, 18). At Z/D = 1 and Z/D = 3 stations, the maximum temperature is achieved near the blowing orifices (Z/D = 1), displaying significant amplitudes, because the jets have not yet merged at this location. Moving in the axial direction, these amplitudes steadily diminish from one station to the next once Z/D > 3, and the irregularities in the curve gradually reduce as well, which suggests that the beginning of thermal stability has occurred. After Z/D = 12, the temperature profiles tend to level off, showing a homogeneous thermal flow. The temperature of the produced jet converges to the component's ambient temperature when seen axially, in the direction of flow, about 18 times the diameter of the jet is present.

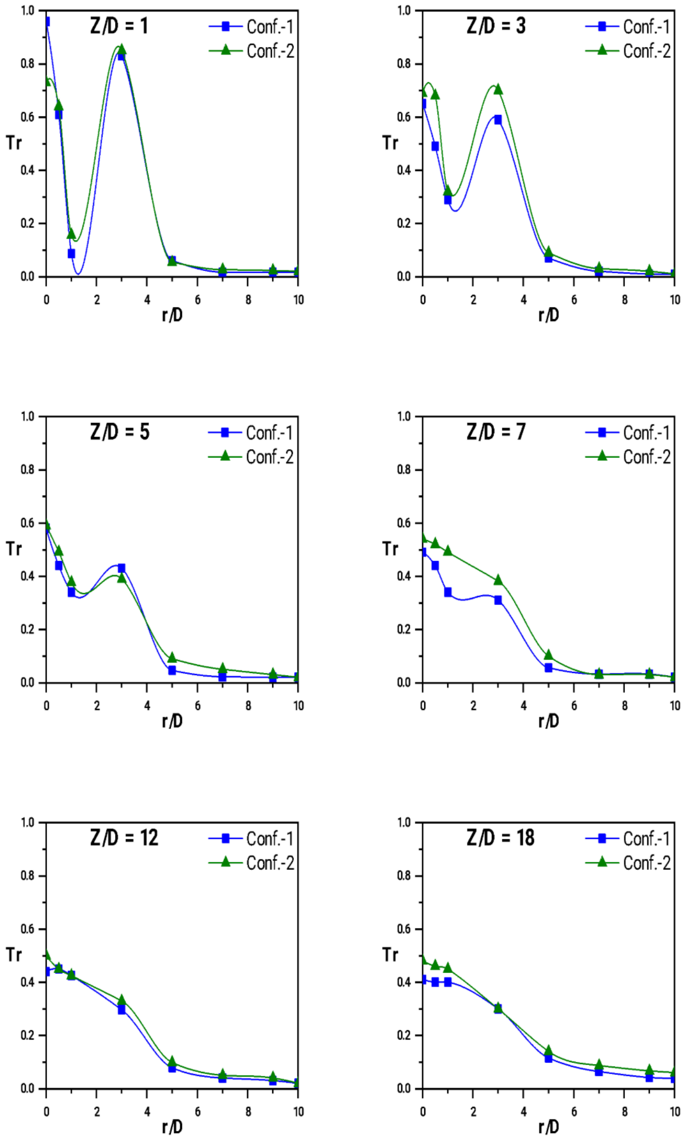

Figure 8. Experimental radial temperature profiles.

Compared to configuration 1, configuration 2 displays a significantly greater expansion in the occupied zone. This expansion becomes particularly clear when seeing the system from Z / D = 5 onwards.

5.4. Numerical results

5.4.1. Velocity and temperature (axial distribution)

Figure 9 and 10 provide a comprehensive comparison of the evolution profiles for temperature and axial velocity, respectively, as calculated by four numerical models (RNG k-ε model, k-ω SST model, RSM model, and k-ω standard model). The analysis reveals that all models show commendable agreement with experimental results in predicting axial velocity and temperature characteristics in the near field. However, a substantial disparity appears in the far field, particularly in the calculated versus measured temperature values. Remarkably, the k-ω SST model stands out as the most correct in predicting flow characteristics, proving consistent alignment with experimental observations at both the close and distant fields. Consequently, the k-ω SST model is chosen as the preferred model to advance numerical study, ensuring a more reliable representation of flow behavior in later analyses.

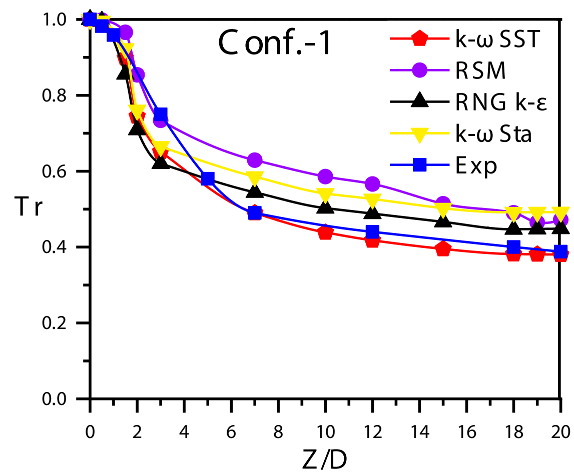

Figure 9. Comparison of axial temperature profiles of configuration 1 from RNG k-ε, k-ω SST, k-ω standard, and RSM models with experimental measurements

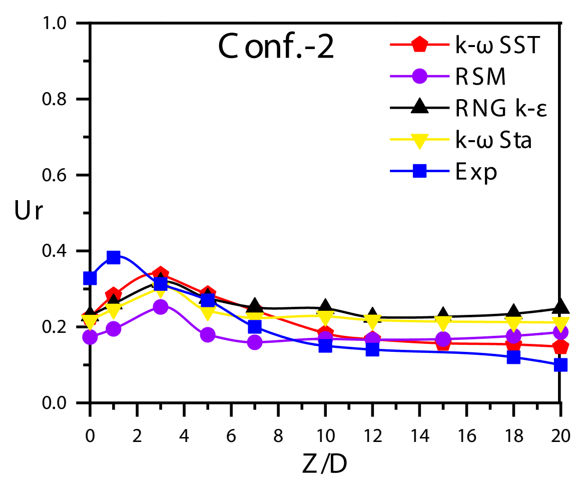

Figure 10. Comparisons of axial velocity profiles for configuration 2 from the RNG k-ε, k-ω SST, k-ω Standard, and RSM models against experimental findings

5.4.2. For the configuration 1 (axial distribution)

The RMSE (Root Mean Square Error) between the k-ω SST model and experimental results for Configuration 1, as shown in Figure 11, is calculated as follows:

For Axial Velocity: RMSE = 0.03682659

For Axial Temperature: RMSE = 0.04733779

These values are the quantitative measure of the disparity between the numerical results of the k-ω SST model and the corresponding experimental data for axial velocity and axial temperature in Configuration 1.

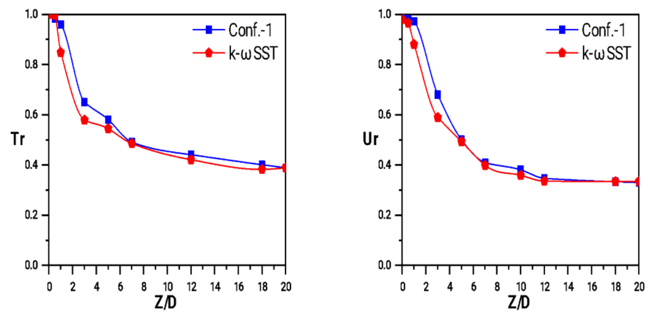

Figure 11. Profiles of axial velocity and temperature, as measured experimentally and computationally for configuration 1

5.4.3. For configuration 2 (axial distribution)

For Configuration 2, the RMSE between the k-ω SST model and experimental results, as depicted in Fig.12, is calculated as follows:

For Axial Velocity: RMSE = 0.05647388

For Axial Temperature: RMSE = 0.03845925

These values quantify the degree of deviation among the numerical simulation of the k-ω SST model and the actual experimental measurements for axial velocity and axial temperature in Configuration 2.

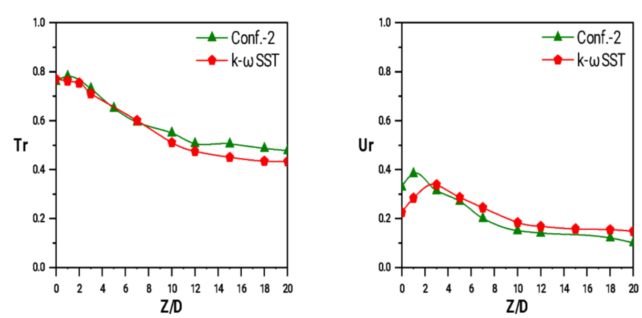

Figure 12. Numerical and experimental velocity and temperature profiles in the axial direction of configuration 2

5.4.4. Velocity and temperature (radial distribution)

5.4.4.1. For the configuration 1

The k-ω SST model has proved remarkable agreement with experimental data concerning primary jets within Configuration 1. To further evaluate its effectiveness, we extend its application to secondary jets, comparing it with experimental results at six distinct positions (Z/D = 1, 3, 5, 7, 12, 18). This assessment includes examining the radial distribution of velocity (Figure 13) and temperature (Figure 14). The results derived from the k-ω SST model reaffirm its suitability for simulating lobed or swirling jets within Configuration 1. It is worth noticing that the model reproduces the experimental data for main and secondary jets rather well. This consistency shows the capability of the model to be the complex flow dynamics associated with these arrangements.

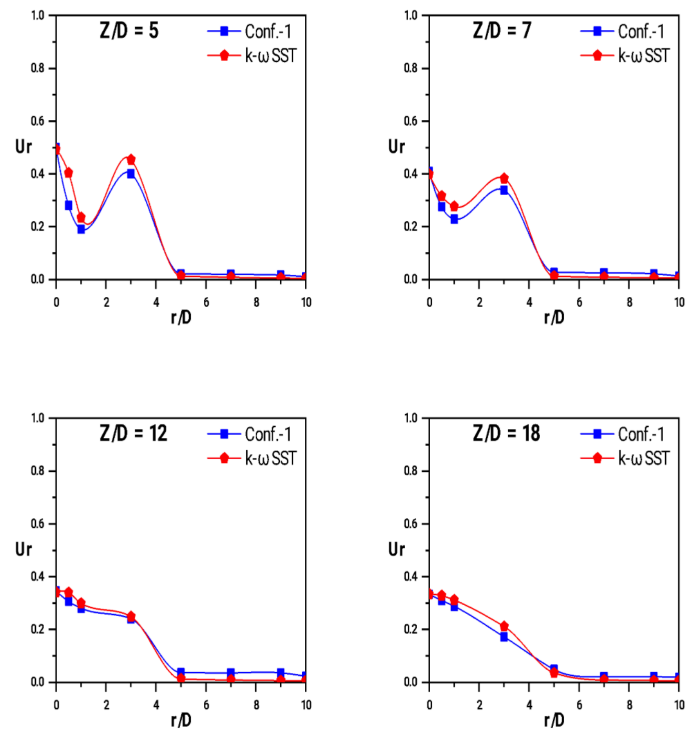

Figure 13. Experimental and numerical radial velocity profiles of configuration 1

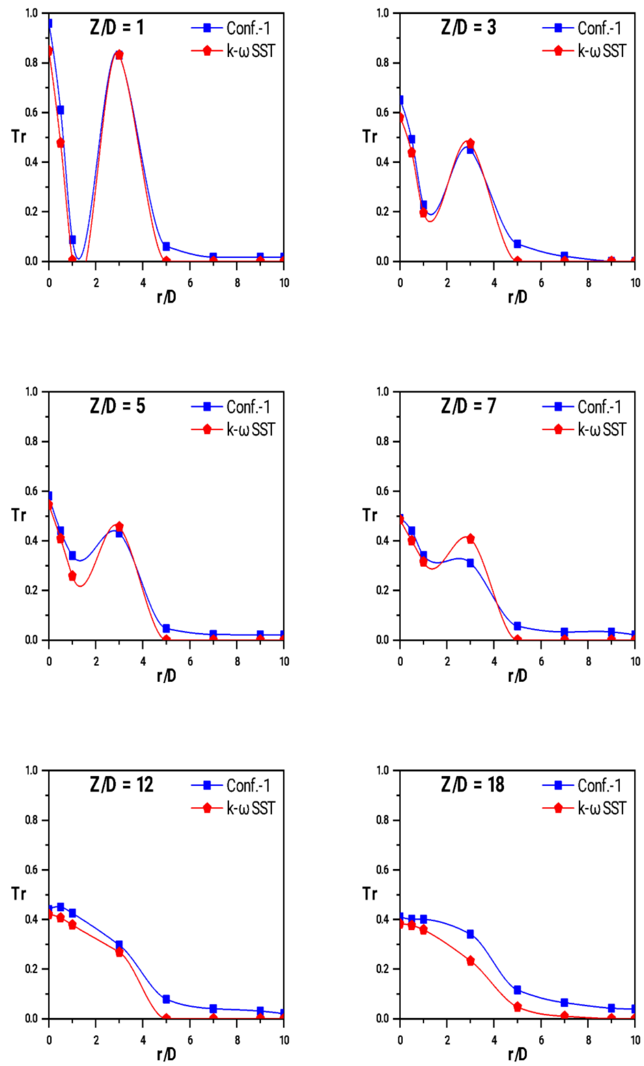

Figure 14. Experimental and numerical radial temperature profiles of configuration 1

Table 3. The RMSE between k-ω SST model and experiment results for configuration 1

	Radial velocity			Radial temperature	
	RMS Error velocity **SST k-ω**			**RMS Error** Temperature **SST k-ω**	
Figure 13	Z/D =1	**0,04780824**	Figure14	Z/D =1	**0,07191923**
	Z/D =3	**0,05130104**		Z/D =3	**0,04322287**
	Z/D =5	**0,05061047**		Z/D =5	**0,0403328**
	Z/D =7	**0,02907035**		Z/D =7	**0,04650716**
	Z/D =12	**0,02239457**		Z/D =12	**0,04246837**
	Z/D =18	**0,01970045**		Z/D =18	**0,05640983**

5.4.4.2. For the configuration 2

Figures (15 and 16) display the measured radial velocity profiles and radial temperature profiles, respectively, for several axial stations selected (Z/D = 1, 3, 5, 7, 12, 18). Notably, the experimental results for swirling and lobed jets closely match the outcomes obtained using the Shear Stress Transport k-ω SST model. This alignment signifies a strong agreement between experimental data and computational simulations, highlighting the efficiency of the k-ω SST model in numerical predicting of the dynamics of swirling and lobed jets.

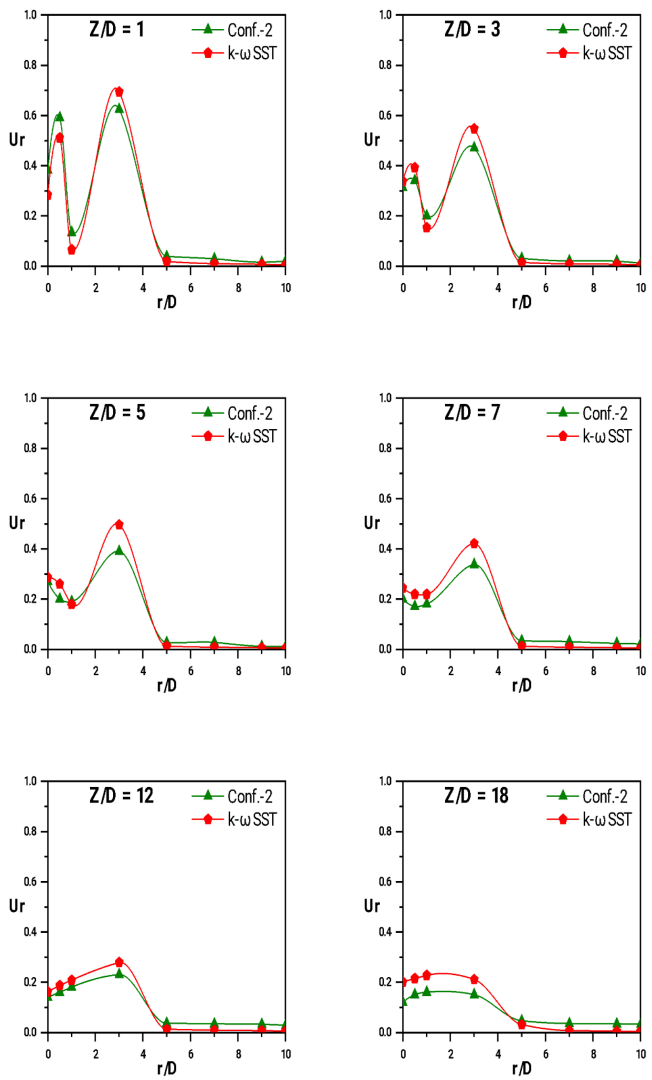

Figure 15. Experimental and numerical radial velocity profiles of configuration 2

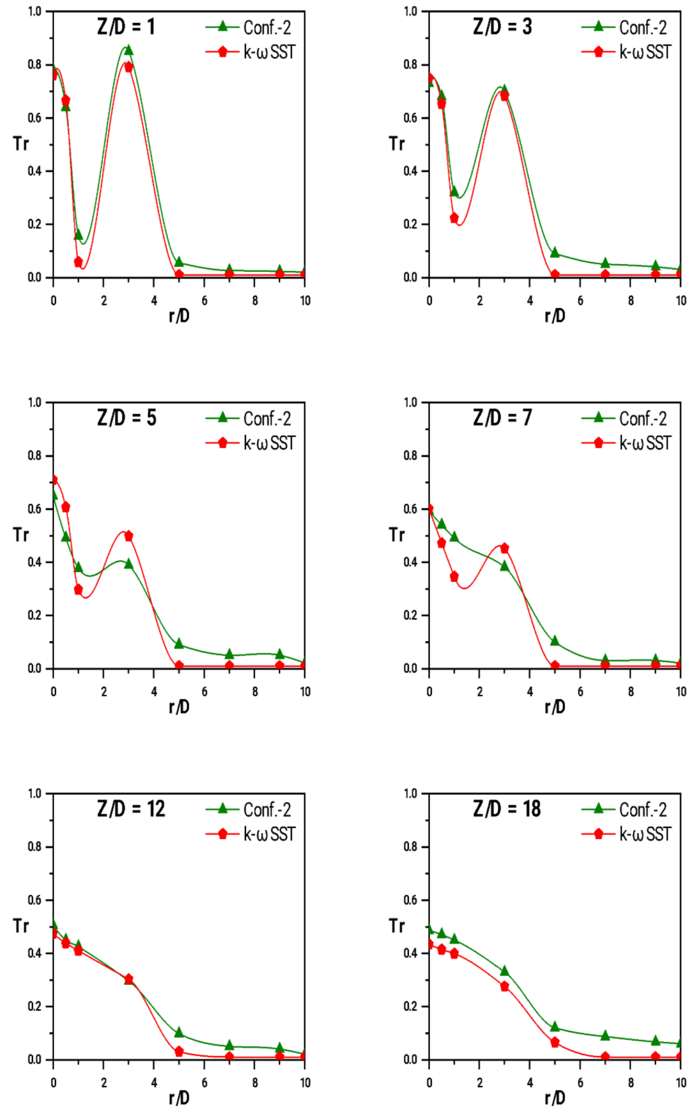

Figure 16. Experimental and numerical radial temperature profiles of configuration 2

Table 4. The RMSE between model k-ω SST and experiment results for configuration 2

	Radial velocity			Radial temperature	
	RMS Error velocity **SST k-ω**			**RMS Error** Temperature **SST k-ω**	
Figure 15	Z/D =1	**0,05822562**	Figure 16	Z/D =1	**0,04591437**
	Z/D =3	**0,038768**		Z/D =3	**0,05008453**
	Z/D =5	**0,0444581**		Z/D =5	**0,07485766**
	Z/D =7	**0,04216271**		Z/D =7	**0,07024845**
	Z/D =12	**0,02890714**		Z/D =12	**0,03296566**
	Z/D =18	**0,05178642**		Z/D =18	**0,05717916**

5.4.4.3. Temperature contours

Figure 17 illustrates the average temperature contours obtained through the k-ω SST model at various axial stations (Z/D = 1, 3, 5, 7, 12, and 18). The experimental observations reveal the presence of three distinct zones. Initially, in the first zone spanning the diameter of the jets' exit, the peripheral jets begin mixing with the surrounding air, converging towards the center jet without mutual interaction. Subsequently, within the second zone delineated between stations Z/D = 3 and Z/D = 12, the jets begin to interact and amalgamate, easing the diffusion of the resultant jet. Finally, extending beyond station Z/D = 12, a third zone appears wherein the temperature profiles show homogeneity, coalescing to form a singular circular jet profile that progresses towards station Z/D = 18. At this juncture, the temperature of the resulting jet approximates that of the ambient air, showing successful homogenization.

5.4.4.4. Velocity contours

Figure 18 presents a detailed view of the temperature iso-contours based on the k-ω SST model at various downstream planes Z/D within the range of 1 to 18. The radial velocities near the blowing device are initially non-uniform but gradually become uniform when they are a certain distance in both radial and axial directions from the radial velocities next to the blowing device are initially heterogeneous but progressively attain uniformity at a certain distance in both radial and axial directions from the outflow jet's surface. This conduct underscores the influence of the lobes' shapes and troughs, that eases relative jet development in the main plane compared to the secondary plane. This phenomenon is seen before reaching station Z/D = 7, identified as the potential core region. Beyond this point, the lobed jet transitions to behave like a circular jet, marking the region where the flow becomes completely developed.

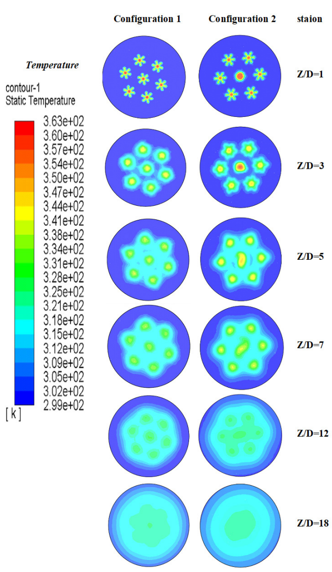

Figure 17. Temperature contours are based on k-ω SST model at different positions

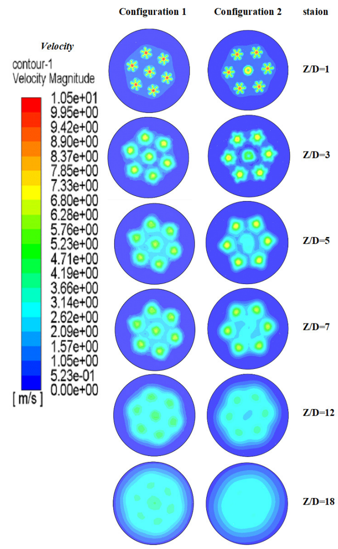

Figure 18. Velocity contours based on k-ω SST model at different positions

5.4.4.5. Specific dissipation rate

For the two configurations under consideration, Figure 19 illustrates the specific dissipation rate plotted against axial distance within the range of Z/D = 1–18. Generally, this quantity shows a trend like that of turbulence energy. However, the decrease in the specific dissipation rate is abrupt from the first stations, distinguishing it from the behavior of turbulence energy. Additionally, the axial developments vary between the two configurations. Comparatively, configuration 2 shows a more substantial reduction in this parameter compared to configuration 1.

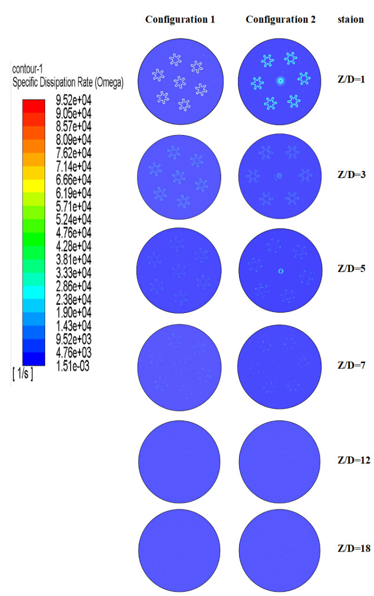

Figure 19. Specific dissipation rate contours based on k-ω SST model at different positions

6. Conclusion

This article describes experiments and simulations of turbulent thermal jets in the form of lobes and swirled intended for use in HVAC. The study aimed to enhance the distribution of air and thermal fields. The optimization process relied on thermal and dynamic predictions, both experimental and numerical, for two diffuser configurations: each featuring six comparable peripheral jets and unique central jet geometry. All configurations had six equidistant peripheral lobed jets, and the central jet was the only distinction between them. Configuration 1 includes a lobed center jet, while Configuration 2 has a swirling central jet. From the results gathered, the later conclusions may be inferred: The axial velocity decreases faster in the second configuration than in the first configuration, which increases the lateral diffusion, leading to better homogeneity. The central jet is crucial in enhancing the mixing process compared with peripheral jets because of its ability to distribute the mixing more uniformly and efficiently throughout the system. The results obtained with the k-ω SST turbulence model showed strong alignment with the experimental findings for both lobed and swirling jets. With correct predictions of flow dynamics and thermal characteristics, the k-ω SST turbulence model has appeared as a suitable tool for swiftly designing best geometrical parameters for lobed and swirling perforated panels in HVC applications. Numerical simulation predictions agree with experimental results on thermal and dynamic fields and the specific dissipation rate evolutions with distance downstream. Ultimately, the integration of optimized diffuser geometries, combined with correct turbulence modeling using the k-ω SST approach, provides a robust foundation for the design of next-generation, energy-efficient HVAC systems that prioritize both comfort and performance. Future extensions could incorporate humidity control, air quality monitoring, or particle dispersion research to provide a more comprehensive understanding of indoor environmental quality. Quantitative results show that the swirling central jet enhances axial dynamic and thermal homogenization by approximately 20%, while radial dynamic and thermal homogenization improve by about 10% compared to the lobed configuration. Additionally, this study proves that the Shear Stress Transport k-ω SST model effectively captures the complex flow structures and thermal behavior of multi-jet diffusers, making it a valuable tool for optimizing the geometric parameters of lobed and swirling perforated panels in heating, ventilation, and air conditioning systems. Furthermore, the k-ω SST model showed superior agreement with experimental results, with Root Mean Square Error values as low as 0.0368 for axial velocity and 0.0384 for axial temperature.

Acknowledgements

LCTMM's head offered the laboratory needed for the study.

Conflict of interest

The authors of this study state that there are no conflicts of interest that are associated with the research, authorship, or publication of this manuscript under consideration.

Authors contribution

Zahout and A. Khelil: Conceptualization, Investigation, reviewing, writing original draft, Editing and Supervision; M. Braikia and H. Naji: Analysis and Reviewing.

Declaration of generative AI and AI-assisted technologies in the writing process

No generative AI or AI-assisted technologies were used in the preparation of this manuscript

Nomenclature

D	Diffuser jet diameter (m)
k	Turbulent kinetic energy (m2.s-2)
P	Pressure (Pa)
Pk	Production of turbulent kinetic energy
Re	Reynolds number
Ta	Ambient temperature
Tr	Dimensionless temperature
T	Wall temperature (K)
Ti	Jet temperature at different stations (K)
Ur	Dimensionless velocity
Ui	Jet velocity at different stations (m.s-1)
r	Radius
SST	Shear Stress Transport
t	Turbulent
μ	Dynamic viscosity, kg.m-1. s-1
ν	Kinematic viscosity (m2.s-1)
ε	Rate of dissipation of turbulent energy (m2.s-3)
ω	Specific dissipation rate (s-1)
ρ	Density (kg.m-3)
θint	Inner penetration angle
θout	Outer Penetration Angle
RNG k-ε	Re-Normalization Group
RSM	Reynolds stress model
k-ω Sta	Standard k-ω model
k-ω SST	Shear stress transport
HVAC	Heating, Ventilation, and Air Conditioning

References

[1] M. Barzegar Gerdroodbary, "Application of neural network on heat transfer enhancement of magnetohydrodynamic nanofluid", Heat Transfer—Asian Res, 49, pp.197–212, 2020. https://doi.org/10.1002/htj.21606.

[2] M. Sheikholeslami, S.A. Farshad, M.B. Gerdroodbary, "Impact of new multiple twisted tapes on treatment of solar heat exchanger ", Eur. Phys. J. Plus, 137, 86,2022. https://doi.org/10.1140/epjp/s13360-021-02157-6.

[3] I.Tlili, R. Moradi, and M. Barzegar Gerdroodbary M, "Transient nanofluid squeezing cooling process using aluminum oxide nanoparticle " ,International Journal of Modern Physics C, 11,pp.1-12,2019. . https://doi.org/10.1142/S0129183119500785

[4] A.M. Abazari, A. Alizadeh, M. Barzegar Gerdroodbary, S. Salavatidezfouli, "Kinetic Energy Harvesters Principles ", Technologies, and Applications, 1st Edition - February 3, 2025. ISBN: 9780443247163.

[5] A. Belhocine, O.I. Abdullah,"Finite element analysis (FEA) of frictional contact phenomenon on vehicle braking system, Mechanics Based Design of Structures and Machines, 50(9), pp.2961–2996,2020. https://doi.org/10.1080/15397734.2020.1787843.

[6] A. Belhocine, O. Wan Zaidi Wan, "Analytical solution and numerical simulation of the generalized Levèque equation to predict the thermal boundary layer", Mathematics and Computers in Simulation, 180,pp. 43-60, 2021. https://doi.org/10.1016/j.matcom.2020.08.007

[7] A. Belhocine, "Numerical study of heat transfer in fully developed laminar flow inside a circular tube", Int JAdv Manuf Technol, 85, pp. 2681–2692, 2016, https://doi.org/10.1007/s00170-015-8104-0

[8] A. Belhocine, W.Z.W. Omar, "Three-dimensional finite element modeling and analysis of the mechanical behavior of dry contact slipping between the disc and the brake pads", Int J Adv Manuf Technol, 88, pp.1035–1051, 2017. https://doi.org/10.1007/s00170-016-8822-y

[9] A. Belhocine,"FE prediction of thermal performance and stresses in an automotive disc brake system".?Int J Adv Manuf Technol 89, pp.3563–3578, 2017. https://doi.org/10.1007/s00170-016-9357-y

[10] A. Belhocine, O.I. Abdullah, "Numerical simulation of thermally developing turbulent flow through a cylindrical tube", Int J Adv Manuf Technol, 102, pp. 2001–2012, 2019. https://doi.org/10.1007/s00170-019-03315-y

[11] A. Belhocine, N. Stojanovic, O.I. Abdullah, "Numerical Simulation of Laminar Boundary Layer Flow Over a Horizontal Flat Plate in External Incompressible Viscous Fluid". European Journal of Computational Mechanics, 30(4-6), PP.337–386, 2021. https://doi.org/10.13052/ejcm2642-2085.30463

[12] A. Meslem, N. Ilinca, A.Francis , "Passive mixing control for innovative air diffusion terminal devices for buildings", Building and Environment, 45(12), pp. 2679-2688,2010. https://doi.org/10.1016/j.buildenv.2010.05.028

[13] N. Ilinca, A. Meslem, "Vortex dynamics and entrainment mechanisms in low Reynolds orifice jets." Journal of visualization, 11(4) pp.309-318, 2008. https://doi.org/10.1007/BF03182199

[14] A. Meslem, N. Ilinca, and K. Abed-Meraim, "Experimental investigation of the mixing performance of a lobed jet flow", Journal of Engineering Physics and Thermophysics, 81(1) pp.106-111,2008. https://doi.org/10.1007/s10891-008-0006-7

[15] B. Sajadi, M. H. Saidi, and A. Mohebbian, "Numerical investigation of the swirling air diffuser: Parametric study and optimization", Energy and Buildings, 43(6) pp.1329-1333, 2011. https://doi.org/10.1016/j.enbuild.2011.01.018

[16] I. Nastase, A. Meslem, I. Vlad, I. Colda, "Lobed grilles for high mixing ventilation–An experimental analysis in a full-scale model room", Building and Environment, 46(3) pp.547-555,2011. https://doi.org/10.1016/j.buildenv.2010.08.008

[17] A. Bennia, L.Loukarfi, M. Braikia, A. Khelil, & H. Naji, "Etude expérimentale d'un jet turbulent à diffuseur muni de lobes: Application au confort dans les locaux à usage d'habitation.", Nature & Technology 13 pp. 5458,226)[18] A. Bennia, L. Loukarfi, A. Khelil, S. Mohamadi, M. Braikia, , & H. Naji, "Contribution to the experimental and numerical dynamic study of a turbulent jet issued from lobed diffuser", Journal of Applied Fluid Mechanics, 9(6)pp. 2957-2967,2016. https://doi.org/10.29252/jafm.09.06.25953

[18] A. Bennia, L. Loukarfi, A. Khelil, S. Mohamadi, M. Braikia, & H. Naji, "Experimental and numerical investigation of a turbulent lobed diffuser jet: Application to residential comfort", Mechanics & Industry, 19(1) pp.104-115, 2018. https://doi.org/10.1051/meca/2016078

[19] K. Xu, G. Wang, L. Wang, F.Yun, W.Sun, X. Wang, &X. CChen, "FD-based study of nozzle section geometry effects on the performance of an annular multi-nozzle jet pump" ,Processes, 8, pp.133-151. https://doi.org/10.3390/pr8020133

[20] M. Draksler, B. Končar, L. Cizelj, & B. Ničeno, "Large Eddy Simulation of multiple impinging jets in hexagonal configuration–Flow dynamics and heat transfer characteristics", International Journal of Heat and Mass Transfer ,109 pp. 16-27, 2017. http://dx.doi.org/10.1016/j.ijheatmasstransfer.2017.01.080

[21] A. Radhouane, I. B. Baouab, N. Mahjoub Saïd, H. Mhiri, P. Bournot, & G. Le Palec, "Temperature impact on the turbulence generated by the interaction of twin inline inclined jets in crossflow", Heat and Mass Transfer, 49 pp. 629-656 (2013). https://ui.adsabs.harvard.edu/link_gateway/2013HMT49629R/doi:10.1007/s00231-012-1108-5

[22] W. Medaouar, L. Loukarfi, M. Braikia, A. Khelil, & H. Naji, "Experimental and numerical study of turbulent multiple jets issued from lobed diffusers", Journal of Applied Fluid Mechanics, 12(3) pp.729-742, 2019. https://doi.org/10.29252/jafm.12.03.29476

[23] B.T. Kannan and N. R. Panchapakesan, "Influence of nozzle configuration on the flow field of multiple jets", Proceedings of the Institution of Mechanical Engineers Part G: Journal of Aerospace Engineering, 232(9) pp. 1639-1654, 2018. https://doi.org/10.1177/0954410017699008

[24] N. K. Depuru Mohan, K. R. Prakash, N. R. Panchapakesan,"Mixing augmentation by multiple lobed jets." American Journal of Fluid Dynamics 5 (2) pp. 55-64, 2015. https://doi.org/10.5923/j.ajfd.20150502.03
[25] B. Pierre, K. Sodjavi, and A. Meslem, "Thermal comfort in heating conditions with a ceiling mounted diffuser comparison of lobed and conventional diffusers", Energy and Buildings, 133, pp.512–528, 2016. https://doi.org/10.1016/j.enbuild.2016.10.023
[26] A. Khelil, H. Naji, L. Loukarfi, H.M. Meliani & M. Braikia, "Numerical simulation of the interactions among multiple turbulent swirling jets mounted in unbalanced positions", Applied Mathematical Modelling, 40(5-6)), pp.3749-3763, 2016. https://doi.org/10.1016/j.apm.2015.10.047
[27] M. Braikia, L. Loukarfi, A. Khelil, & H. Naji, "Improvement of thermal homogenization using multiple swirling jets", Thermal science ,16 (1) pp.239-250, 2012. http://dx.doi.org/10.2298/TSCI101026131B
[28] D.C. Wilcox, "Turbulence Modeling for CFD", DCW Industries, La Canada, CA, USA. (2006).
[29] C. W. David, "Formulation of the kw turbulence model revisited", AIAA journal ,46 (11), pp.2823-2838,2008.
[30] D. Choudhury, "Introduction to the renormalization group method and turbulence modeling", Technical Memorandum TM-107, Fluent Inc. 1993). http://dx.doi.org/10.4314/jfas.v6i1.10
[31] V. Yakhot; S. A. Orszag; S. Thangam; T. B. Gatski; C. G. Speziale,"Development of turbulence models for shear flows by a double expansion technique", Phys. Fluids, 4, pp.1510–1520, 1992. https://doi.org/10.1063/1.858424
[32] F. Menter,"Zonal two equation kw turbulence models for aerodynamic flows", 23rd fluid dynamics, plasmadynamics, and lasers conference. 1993. https://doi.org/10.2514/6.1993-2906
[33] F. Menter, "Two-equation eddy-viscosity turbulence models for engineering applications.", AIAA journal 32(8), pp. 1598-1605,1994. https://doi.org/10.2514/3.12149
[34] F. Menter,"Review of the shear-stress transport turbulence model experience from an industrial perspective", International journal of computational fluid dynamics, 23(4) pp. 305-316,2009. https://doi.org/10.1080/10618560902773387
[35] N. Zahout, M. Braikia, A. Khelil, H. Naji, "Thermal and dynamic characterization of a multi-jet system with different geometry diffusers", Journal of Thermal Engineering, 10(2) pp. 404–429, 2024, https://doi.org/10.18186/thermal.1456643
[36] A. Fellague Chebra, A. Khelil, M. Braikia, M. Bedrouni, "Comparative analysis of modified jet diffuser geometry for evaluating the impact of rounded edges and chamfered design on cooling efficiency of electronic components in cross flow and impinging jet", Journal of Thermal Engineering, 10 (4) pp. 961– 977,2024, https://doi.org/10.14744/thermal.0000849
[37] M. S.Illyas, B. R.Ramesh Bapu, A. Muthu Manokar, "Experimental and Computational Study of Heat Transfer and Flow Structure of Slotted Impinging Jet ", Journal of Thermal Engineering, 10(5) pp. 1275-1291, 2024. https://doi.org/10.14744/thermal.0000866
[38] S. Atheer Hmaizah, M. Alaa Abbas, M. Wahhab Aljibory, "Experimental and Numerical Study for Assessment Indoor Air Quality by Adopting Mixing Ventilation with Different Occupants Density in Iraq Hot Climates", Journal of Thermal Engineering, 10(I2) pp.430-446, 2024, https://doi.org/10.18186/thermal.1456666
[39] M. Bedrouni, A. Khelil, "Numerical study on the performance of rounded corners on the top of electronic components on cooling effectiveness " , International Journal of Heat and Mass Transfer, 150, , 119391, 2020. https://doi.org/10.1016/j.ijheatmasstransfer.2020.119391
[40] ANSYS Fluent Theory Guide (2020), ANSYS Inc., USA. (2020).